IBRO Neuroscience Reports 12 (2022) 90–97

Contents lists available at ScienceDirect

IBRO Neuroscience Reports

journal homepage: www.sciencedirect.com/journal/IBRO-Neuroscience-Reports

CaMKIIβ knockdown decreases store-operated calcium entry in hippocampal dendritic spines

Nikita Zernov [a], Ilya Bezprozvanny [a,b], Elena Popugaeva [a,*]

[a] Peter the Great St.Petersburg Polytechnic University, Laboratory of Molecular Neurodegeneration, St.Petersburg, Russia
[b] UT Southwestern Medical Center, Department of Physiology, Dallas, USA

ARTICLE INFO

Keywords:
Store-operated calcium entry
Calcium/calmodulin-dependent protein kinase II
Calcium imaging

ABSTRACT

Calcium/calmodulin-dependent protein kinase II (CaMKII) and neuronal store-operated calcium entry (nSOCE) have been implicated in the development of Alzheimer's disease (AD). nSOCE is involved in regulation of dendritic spine shape, particularly in stability of mushroom spines that play role in formation of strong synapses. CaMKII is involved in regulation of induction of long-term potentiation, that is needed for shaping of memory. In the present study, we demonstrated that inhibition of kinase activity of CaMKII by KN-62 decreases nSOCE amplitude in soma of primary hippocampal neurons. We have shown that knockdown of CaMKIIβ leads to the downregulation of nSOCE in dendritic spines. In agreement with previously published data, we have also observed that CaMKIIβ knockdown causes mushroom spine loss in primary hippocampal culture. The effect of CaMKIIβ knockdown on the nSOCE may be associated with a decrease of dendritic spine head size.

1. Introduction

AD is the most common form of dementia in the world. AD is characterized by synaptic dysfunction and neuronal death that leads to slowly progressing memory loss and gradual decline in cognitive function. The disease remains incurable, mostly because of its complex etiology (Castellani and Perry, 2012). Multiple studies suggest that calcium dysregulation is involved in the development of the disease (LaFerla, 2002; Supnet and Bezprozvanny, 2010). Endoplasmic reticulum (ER) calcium level of the neuronal cells is elevated in AD (Emilsson et al., 2006; Ito et al., 1994). We have previously shown that elevated ER calcium levels in hippocampal neurons lead to the downregulation of neuronal store-operated calcium entry (nSOCE) (Sun et al., 2014). nSOCE in hippocampal neurons plays a critical role in stability of mushroom spines (places of strong synaptic contacts), the loss of which is indicative of a deficiency in synaptic connections (Ryskamp et al., 2019; Sun et al., 2014). As a consequence of nSOCE downregulation dendritic spines are eliminated in various in vitro and in vivo models of AD (Popugaeva et al., 2015; Sun et al., 2014; Zhang et al., 2015).

In neurons nSOCE is regulated by tripartite complex. This complex consists of stromal interaction molecules (STIM1 or STIM2) which act as ER calcium sensor and plasma membrane channel: proteins from ORAI and TRPC family. Although STIM1 role in regulation of nSOCE have been documented by several research groups (Gruszczynska-Biegala et al., 2011; Klejman et al., 2009; Ng et al., 2011; Skibinska-Kijek et al., 2009; Vlachos et al., 2009), we detect dysfunction of STIM2-ORAI2-TRPC6 tripartite complex in different cellular models of Alzheimer's disease (Popugaeva et al., 2015; Sun et al., 2014; Zhang et al., 2016). In response to ER Ca^{2+} depletion STIM2 starts to oligomerize and moves to ER-plasma membrane tight junctions where it interacts with Orai2 and TRPC6 in order to allow Ca^{2+} influx from extracellular space (Zhang et al., 2016). We have previously suggested that in neurons nSOCE downstream intracellular signaling pathway is based on pCaMKII activation, that is needed to support long-term potentiation (LTP) in silent synapses and preserve plasticity and memory storage (Popugaeva et al., 2018). Indeed we have previously observed downregulation of pCaMKII expression in primary hippocampal neurons as well as in the hippocampus from AD mouse models (Popugaeva et al., 2015; Sun et al., 2014; Zhang et al., 2016). Upregulation of nSOCE via overexpression of STIM2 or TRPC6 caused recovery of pCaMKII protein expression levels in KI AD model (Sun et al., 2014) and in amyloid toxicity model (Popugaeva et al., 2015) as well as increase of mushroom spine percentage (Popugaeva et al., 2015, 2019; Sun et al., 2014; Zhang et al., 2016). In addition, we have observed that pharmacological upregulation of TRPC6 dependent nSOCE caused recovery of long-term potentiation (LTP) in brain slices from APP-KI

* Corresponding author.
E-mail address: lena.popugaeva@gmail.com (E. Popugaeva).

https://doi.org/10.1016/j.ibneur.2022.01.001
Received 20 September 2021; Received in revised form 6 January 2022; Accepted 8 January 2022
Available online 10 January 2022

(Zhang et al., 2016) and 5xFAD models (Popugaeva et al., 2019). In non-excitable cells it has been shown that TRPC6 has two spatially separated CaMKII phosphorylation sites. TRPC6 phosphorylation by CaMKII may mediates positive regulation of channels in response to calcium entry (Shi et al., 2013). Moreover, podocyte-specific TRPC6 transgenic mice showed CaMKII activation, whereas TRPC6 null mice exhibited reduced CaMKII activation and higher levels of proteinuria compared with wild type littermates (Kistler et al., 2013). However, experimental observation of CaMKII activation in response to nSOCE stimulation in neurons has not been published so far.

Thus, within the current paper we investigate whether CaMKII plays role in regulation of nSOCE activity in primary hippocampal neurons and discuss possible cellular mechanisms of CaMKII-dependent nSOCE regulation.

2. Experimental procedures

2.1. Mice

Albino inbred mice (FVB/NJ) were obtained from the Jackson Laboratory (Stock No: 001800) and used as a source of brain tissue for the experiments with hippocampal cultures.

2.2. KN-62

KN-62 (4-[(2 S)− 2-[(5-isoquinolinylsulfonyl)methylamino]− 3-oxo-3-(4-phenyl-1-piperazinyl)propyl] phenyl isoquinolinesulfonic acid ester) is a cell-permeable inhibitor of all CaMKII subunits. KN-62 was purchased from Tocris (Tocris #1277).

2.3. Plasmids

pCSCMV:tdTomato plasmid was a gift from Gerhart Ryffel (Addgene #30530) (Waldner et al., 2009). Venus-CaMKIIα was a gift from Steven Vogel (Addgene #29428) (Thaler et al., 2009). GFP-C1-CAMKIIbeta (GFP-CaMKIIβ) was a gift from Tobias Meyer (Addgene #21227) (Shen et al., 1998). CaMKIIβ shRNA (shCaMKIIβ) plasmid was obtained from Santa Cruz Biotechnology (#sc-38951-SH). Control short hairpin RNA interference (shControl) was obtained from Sigma (#SHC002).

2.4. Primary hippocampal neuronal cultures

The hippocampal cultures from FVB/NJ mice were established from postnatal day 0–2 pups and maintained in culture as described previously (Chernyuk et al., 2019; Popugaeva et al., 2015; Sun et al., 2014).

Briefly, hippocampus was dissected in sterile ice-cold dissection buffer (1% 10x CMF-HBSS (Gibco, #14185), 1% Pen Strep (Gibco, #15140), 1.6 MM HEPES (Sigma, #H3375), 1 MM NaHCO3 (Sigma, #S5761); pH = 7.6). After that it was digested with papain solution (Worthington, #LK003176) 30 min at 37 °C, then twice triturated with 5 mg/ml DNase I solution (Sigma, #DN-25). Neurons were plated in 24-well culture plate on 12 mm glass coverslips (Thermo Scientific, #CB00120RA1) precoated with 0.1 mg/ml poly-D-lysine (Sigma, #P0899) in Neurobasal (Gibco, #10888) medium supplemented with 1% FBS (Gibco, #10500), 2% 50xB27 (Gibco, #17504), 0.05 MM L-Glutamine (Gibco, #250030) and maintained at 37 °C in a 5% CO2 incubator. A half of the medium was replaced with a new culture medium at DIV 7 and DIV 14.

2.5. HEK293T cultures

Cell line HEK293T (Human embryonic kidney 293) contains the SV40 T-antigen, that makes them highly transfectable. Cells were cultured on sterile coverslips at 37 °C in a humidified atmosphere of 5% CO_2 in air in DMEM (Gibco, #41965) with 10% FBS (Gibco, #10500), 1% PEST, (Gibco, #15140), 1% Sodium Pyruvat (Gibco, #11360), 1% MEM NEAA (Minimum Essential Medium Non-Essential Amino Acids, Gibco, #11140).

2.6. Calcium phosphate transfection of primary hippocampal cultures

Primary hippocampal neurons were transfected using the calcium phosphate method as previously described (Sun et al., 2014). Alterations to the original protocol are the following: the volume of transfection reaction added to each well was 25 μl and conditioned medium was not replaced by serum free medium. Transfection kit was obtained from Clontech (TAKARA Biotechnology #631312).

2.7. Western Blot analysis

HEK293T line cells were co-transfected with Venus-CaMKIIα or GFP-CaMKIIβ with shControl or shCaMKIIβ plasmids using polyethylenimine reagent (Polyscience, #23966) in 1:1 ratio. Co-transfected cells were homogenized in RIPA lysis buffer (50 mM Tris-HCl, 150 mM NaCl, pH 7.5, 0.1% sodium dodecyl sulfate, 0.5% sodium deoxycholate, 1% NP-40, 1 mM PMSF, protease (Sigma, #S8820) and phosphatase (Sigma, #P0044) inhibitors) on the next day. The total protein lysates were electrophoreticly separated by size on sodium dodecyl sulphate (SDS) polyacrylamide gel. Separated proteins were immobilized to the nitrocellulose membrane. Non-specific proteins on the membrane were blocked by incubation of the membrane in 5% bovine serum albumin (BSA) (Sigma, #A9430) in TBST (tris-buffered saline and Tween 20: 50 MM Tris, 150MM NaCl, 0.1% Tween 20, pH = 7.6). Target proteins were detected with anti-green fluorescent protein (1:1000, Invitrogen, #A11122), anti-tubulin (1:1500, DSHB, E7-c) and horseradish peroxidase-conjugated anti-rabbit (1:2000, DAKO, P0448) and anti-mouse (1:2000, DAKO, #P0447) secondary antibodies. Increase of HRP luminescence is achieved using ECL buffer (enhanced chemiluminescence): 9 ml ddH2O, 1.5 ml 1 M Tris-HCl (pH = 8.8), 50 ul luminol [44 mg / ml], 22 ul paracumarate [15 mg / ml] 70 ul 3% H2O2. The enhanced luminescence was recorded on X-ray film.

2.8. Immunochemistry

Neurons were washed with PBS, fixed with 4% paraformaldehyde in PBS, pH 7.3, for 10–15 min at room temperature and permeabilized in 0.05% Tween20 for 5 min at room temperature. Nonspecific binding was blocked with 5% BSA in PBS solution for 1 h. Then cells were incubated with anti-MAP2 (1:1000, Millipore, #MAB378) and anti-pCaMKII (1:1000, Cell Signaling, #33613) primary antibodies diluted in 2.5% BSA in PBS at 4 °C overnight. After three washing cycles in PBS, cells were incubated in 2.5% BSA in PBS solution with anti-rabbit (Alexa Fluor 594, 1:1000, Invitrogen, #A11012) and anti-mouse (Alexa Fluor 488, 1:1000, Invitrogen, #A11001) for 1 h at room temperature and then washed three times in PBS and visualized by a confocal microscope (ThorLabs).

2.9. Dendritic spine analysis in primary hippocampal neuronal cultures

For assessment of synapse morphology, hippocampal cultures were co-transfected with TD-tomato plasmid and shCaMKIIβ or shControl plasmids in 1:1 ratio at DIV7 using the calcium phosphate method and then fixed with 4% paraformaldehyde in PBS, pH 7.4, at DIV14 – 16.

A Z-stack of 8 – 10 optical sections with 0.2 μm interval was captured using a 100 × lens (UPlanSApo, 100x/1.40 Oil, OLYMPUS) with a confocal microscope (Thorlabs). Each image was captured at 1024 × 1024 pixels with maximum resolution 0.1 μm/pixel. At least 10 transfected neurons of each group from three independent experiments were used for quantitative analysis.

Morphological analysis of dendritic spines was performed by using the freely available NeuronStudio software package (Rodriguez et al., 2008) as previously described (Sun et al., 2014). In the classification of

spine shapes we used the following cutoff values: aspect ratio for thin spines = 2.5, head-to-neck ratio = 1.4, and head diameter = 0.45 μm. Spine density was measured as the ratio of the number of spines to the length of the analyzed part of dendrite.

2.10. Calcium imaging

Calcium imaging was performed one week after transfection or at DIV 14.

Calcium imaging was performed using a green-fluorescent calcium indicator Fluo4 AM (Invitrogen, #F14201) or genetically encoded calcium indicator GCamp5.3. In the first case, primary hippocampal neuronal culture was incubated in ACSF (artificial cerebrospinal fluid: 140 mM NaCl, 5 mM KCl, 10 mM HEPES, 1 mM MgCl2, 2 mM CaCl2) with Fluo4 AM for 30 min and washed in ACSF for 20 min at room temperature. This step was not necessary in GCamp5.3 calcium imaging experiments.

At DIV14 GCaMP5.3 or Fluo4 live fluorescent images were collected every 2 s using Olympus IX73 confocal microscope with 40x lens (LUMPlanFL N, 40 ×/0.80 Water, OLYMPUS) under control of Micro-Manager 2.0 (Vale Lab, UCSF).

Neurons were incubated in calcium-free ACSF (140 mM NaCl, 5 mM KCl, 10 mM HEPES, 1 mM MgCl2, 100 uM EGTA) for recording basal fluorescent signals. Then ACSF was replaced by 300 ul calcium-free ACSF with drugs (10 uM D-Ap5 (Tocris, #0106), 50 uM nifedipine (Tocris #1075), 10 uM CNQX (Tocris, #0190), 1 uM tetrodotoxin (TTX) (Tocris, #1078), 1 uM thapsigargin (Tg) (Tocris, #1138)) for the same time for all experiments. nSOCE was induced by puff application of 3 ul of 200 mM $CaCl_2$ so the resulting calcium concentration in the cuvette was 2 mM.

Analysis of the data was performed using ImageJ software. The ROI used in the image analysis was chosen to correspond to spines (GCaMP) or somas (Fluo 4), and signal was normalized to baseline.

2.11. Statistical analyses

The results are presented as mean ± SEM. Statistical comparisons of the results were performed by Student's t-test for two-group comparisons. The P values are indicated in the text and figure legends as appropriate.

3. Results

3.1. KN-62 reduces pCaMKII expression in hippocampal neurons

KN-62 is an inhibitor of all subunits of CaMKII. It inhibits enzyme autophosphorylation and phosphorylation of substrates by binding to the calmodulin binding site of CaMKII (Tokumitsu et al., 1990).

The inhibition of CaMKII in neurons of the primary hippocampal culture was determined by immunofluorescence analysis. The culture was incubated overnight with 10 uM KN-62 at DIV 13. Then it was fixed and stained on the next day. Mean fluorescence intensity of pCaMKII

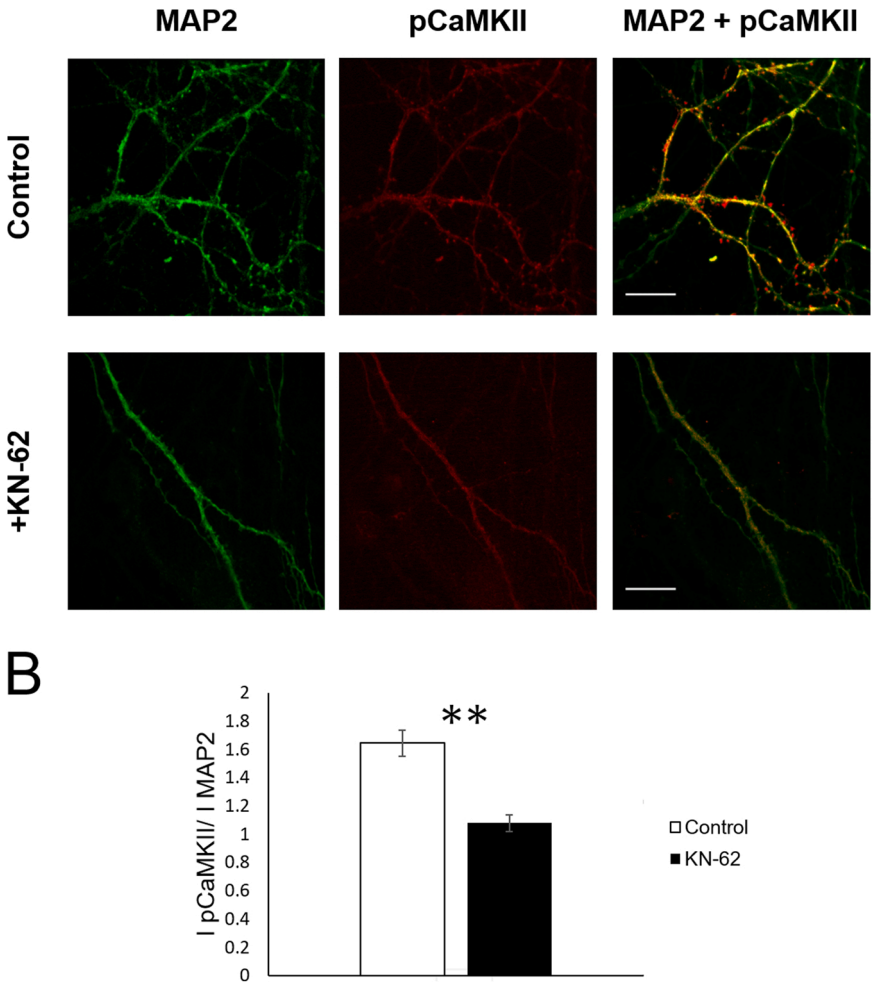

Fig. 1. KN-62 inhibits pCaMKII activity in hippocampal neurons. (A) Confocal images of dendrites of hippocampal neurons stained for MAP2 and pCaMKII. (B) Quantitative analysis of pCaMKII fluorescence intensity (pCaMKII fluorescence intensity normalized to MAP2 fluorescence intensity). Results are presented as mean ± SEM. Statistical analysis was performed using Student's t-test, ** $p < 0.001$ ($n = 10$ for each group). Scale bar = 20 μm.

was normalized with mean fluorescence intensity of MAP2 to quantify the level of pCaMKII inhibition. The staining results are shown in Fig. 1. Quantitative analysis showed a decrease in fluorescence intensity of the active form of enzyme (pCaMKII) by more than 30%: from 1.64 ± 0.09 a. u. in the control group down to 1.08 ± 0.06 a. u. in the group with KN-62 ($p < 0.005$) (Fig. 1B).

These results prove that KN-62 inhibits the enzyme activity in hippocampal neurons. The same results are shown for 2-[N-(2-hydroxyethyl)]-N-(4-methoxybenzenesulfonyl)amino-N-(4-chlorocinnamyl)-N-methylbenzylamine (KN-93) (Redondo et al., 2010).

3.2. KN-62 causes a decrease in nSOCE in the soma of primary hippocampal neurons

The exact role of CaMKII in regulation of SOCE is unknown. Nevertheless, the recent studies revealed that inhibition of all subunits of CaMKII with KN-93 downregulates SOCE in HEK293 and HeLa cells (Li et al., 2018).

Our goal was to investigate how KN-62 effects nSOCE in hippocampal neurons of wild-type mice by calcium imaging using the Fluo4 AM indicator dye. Fluo4 is a popular calcium indicator. When bound with calcium, it is capable of increasing the quantum response by more than 100 times.

KN-62 was added to the neurons at a concentration of 10 uM at DIV10. The culture was incubated overnight, and the experiment was carried out on the next day. The experimental results are shown in Fig. 2. Fluo 4 stains only somas of neurons, so in the representative graphs (Fig. 2 (A)) each gray curve corresponds to the value of one neuron.

We have observed that KN-62 decreases nSOCE amplitude in hippocampal neurons (Fig. 2 (B)), demonstrating nSOCE peak amplitude 2.27 ± 0.09 a.u. (n (neurons) = 97) in the KN-62 group versus 4.23 ± 0.12 a.u. (n (neurons) = 133) in the control group, $p < 0.0001$. Considering the fact that during the experiment the imaging solution contains blockers of powerful calcium permeable channels, such as NMDAR, AMPAR, VGCC, SERCA, the recording of the increase in Fluo 4 fluorescence corresponds to the entry of calcium through the ER-controlled channels. This allows us to conclude that nSOCE is decreased by more than 50% in the presence of KN-62.

3.3. Specificity and effectiveness of CaMKIIβ knockdown by short hairpin RNA

There are 4 isoforms of CaMKII: α, β, δ and γ. The δ and γ isoforms are expressed in various tissues, including the brain, while the α and β are predominant isoforms for the brain (Bennett et al., 1983; Tobimatsu & Fujisawa, 1989). It was demonstrated that β, δ and γ of CaMKII subunits can bind to F-actin, which modulates dendritic spine shape (Hoffman et al., 2013; O'Leary et al., 2006). However, only impairment of CaMKIIβ function leads to the changes in the spine shape, knockdown of CaMKIIα does not influence spine's morphology (Okamoto et al., 2007). Thus, investigation of the role of CaMKIIβ in terms of nSOCE-mediated mushroom spines dysfunction in hippocampal neuron looks reasonable. Since KN-62 treatment inhibits all subunits equally we focused following up experiments on usage beta subunit-specific shRNA-mediated knockdown of CaMKII (shCaMKIIβ).

The specificity and effectiveness of CaMKIIβ inhibition were determined using the Western blot method. HEK293T cells were divided into four groups. Each group was co-transfected with an individual

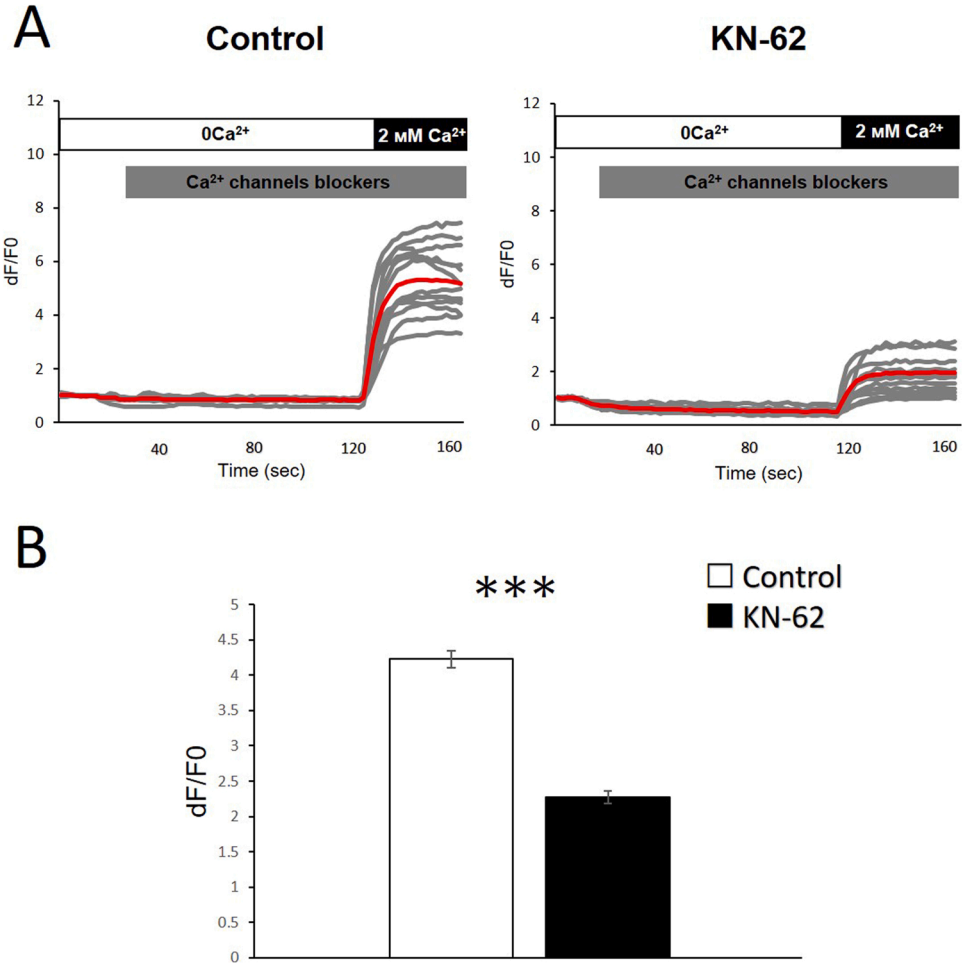

Fig. 2. KN-62 decreases store-operated calcium entry in soma of primary hippocampal cultures. (A) Time course of Fluo 4 relative fluorescence signal changes (F/F0) in individual soma of hippocampal neuron. Presence of Ca^{2+} channels blockers (Tg, TTX, Nifedipine, D-AP5,CNQX) is indicated by grey bars. The time of extracellular Ca^{2+} readdition is indicated by a black bar above the traces. Neurons were incubated in the presence or absence of 10 uM KN-62 for a night. For each experimental group, individual neuron (gray) and average (red) fluorescence traces are shown. (B) Average nSOCE peak amplitude is shown for each group of cells shown in panel A. Mean F/F0 peak amplitude signals for each group are presented as mean ± SEM ($n \geq 107$ neurons from 3 independent experiment). Statistical analysis was performed using Student's t-test, *** $p < 0.0001$.

combination of plasmids, which are the following: Venus-CaMKIIα + shControl, Venus-CaMKIIα + shCaMKIIβ, GFP-CaMKIIβ + shControl, GFP-CaMKIIβ + shCaMKIIβ. The ratio of TD-Tomato:shRNA (1:1) was determined empirically (higher ratios as 1:2 or 1:3 caused cross-specific knockdown of CaMKIIα, Supplementary Fig. 1). The day after co-transfection, lysates were prepared from the cells. Membranes were stained for tubulin and GFP. The expression level of the fluorescent protein in each of the groups was analyzed.

shCaMKIIβ plasmid carries a small hairpin RNA sequence that suppresses CaMKIIβ expression. According to our results, shCaMKIIβRNA is highly specific.

Expression level of CaMKIIβ was downregulated by 94 ± 2% ($P < 0.05$) for the group co-transfected with GFP-CaMKIIβ + shCaMKIIβ plasmids as compared to the control group co-transfected with GFP-CaMKIIβ + shControl plasmids (Fig. 3 B and D). In contrast, expression levels of CaMKIIα in groups co-transfected with Venus-CaMKIIα + shCaMKIIβ or shControl plasmids remained unchanged (Fig. 3 A and C).

3.4. *CaMKIIβ knockdown decreases mushroom spine percentage in hippocampal neurons*

Dendritic spines, small membrane protrusions on dendrites, form the postsynaptic compartment of excitatory synapses. There are three traditional classes of spines: mushroom, thin and stubby.

Mushroom spines, the ones with large head and thin neck, are considered to be responsible for memory formation and learning processes (Bourne and Harris, 2007; Hayashi and Majewska, 2005). They have larger postsynaptic density (PSD) then other types which help them form strong synaptic connections (Helm et al., 2021). A decrease in mushroom spines makes these synapses functionally weaker which leads to cognitive impairment (Tackenberg et al., 2009). AD is known to be accompanied by mushroom spine shrinkage in the hippocampus (Boros et al., 2017; Tackenberg et al., 2009). Thin spines are considered to be young learning spines. These spines have a structure similar to the mushroom spines, but their small heads are separated from the dendrite by long necks. Spine necks are plastic structures that become wider and shorter after long-term potentiation (Tønnesen et al., 2014). Stubby spines, the smallest ones, typically do not have a neck. Using electron microscopy, it was showing that stubby spines indeed are much less common then they are reported in the light microscopic literature due to insufficient optical resolution (Tønnesen et al., 2014). We have used confocal microscopy in order to study spine morphology, thus we allow an error in the quantification of stubby spine.

To investigate the role of CaMKIIβ in maintaining the structure of dendritic spines primary hippocampal culture was co-transfected with TD-Tomato and shCaMKIIβ or shControl plasmids at DIV 7. The ratio of TD-Tomato:shRNA was 1:1 (higher ratios as 1:2 or 1:3 caused cross-specific knockdown of CaMKIIα, Supplementary Fig. 1). The culture was fixed a week after transfection.

We have observed that CaMKIIβ knockdown causes decrease in mushroom spine percentage from 31.54% ± 1.19% in the control group (Fig. 4 A, B) to 15.30% ± 1.28% in the shCaMKIIβ group (Fig. 4 A, B), $n \geq 27$ neurons from 4 batches of cultures, $P < 0.0001$. The number of stubby spines was also reduced from 32.50% ± 1.86% in the control group to 17.17% ± 1.26% in the group with CaMKIIβ knockdown, $n \geq 27$ neurons from 4 batches of cultures, $P < 0.0001$. Meanwhile thin spines percentage increases, 35.67% ± 1.67% in the control group versus 67.52% ± 1.74% in the group with CaMKIIβ knockdown, $n \geq 27$ neurons from 4 batches of cultures, $P < 0.0001$.

We have observed that CaMKIIβ knockdown causes decrease in mushroom spine percentage from 31.54% ± 1.19% in the control group (Fig. 4 A, B) to 15.30% ± 1.28% in the shCaMKIIβ group (Fig. 4 A, B), $n \geq 27$ neurons from 4 batches of cultures, $P < 0.0001$. The percentage of stubby spines was also reduced from 32.50% ± 1.86% in the control group to 17.17% ± 1.26% in the group with CaMKIIβ knockdown, $n \geq 27$ neurons from 4 batches of cultures, $P < 0.0001$. Meanwhile thin spine percentage increases, 35.67% ± 1.67% in the control group versus 67.52% ± 1.74% in the group with CaMKIIβ knockdown, $n \geq 27$ neurons from 4 batches of cultures, $P < 0.0001$.

We have also observed that CaMKIIβ knockdown causes a reduction in mushroom spine density from 0.10 ± 0.01 spines/um in the control group (Fig. 4, C) to 0.06 ± 0.01 spines/um in the shCaMKIIβ group (Fig. 4, C), $n \geq 27$ neurons from 4 batches of cultures, $P < 0.05$. The stubby spine density was reduced as well from 0.10 ± 0.01 spines/um in the control group to 0.05 ± 0.01 spines/um in the group with CaMKIIβ knockdown, $n \geq 27$ neurons from 4 batches of cultures, $P < 0.0001$. Meanwhile thin spine density increases, 0.12 ± 0.01 spines/um in the control group versus 0.27 ± 0.02 spines/um in the group with CaMKIIβ knockdown, $n \geq 27$ neurons from 4 batches of cultures, $P < 0.0001$ (Fig. 4 C).

Our results are consistent with the previous studies of CaMKIIβ

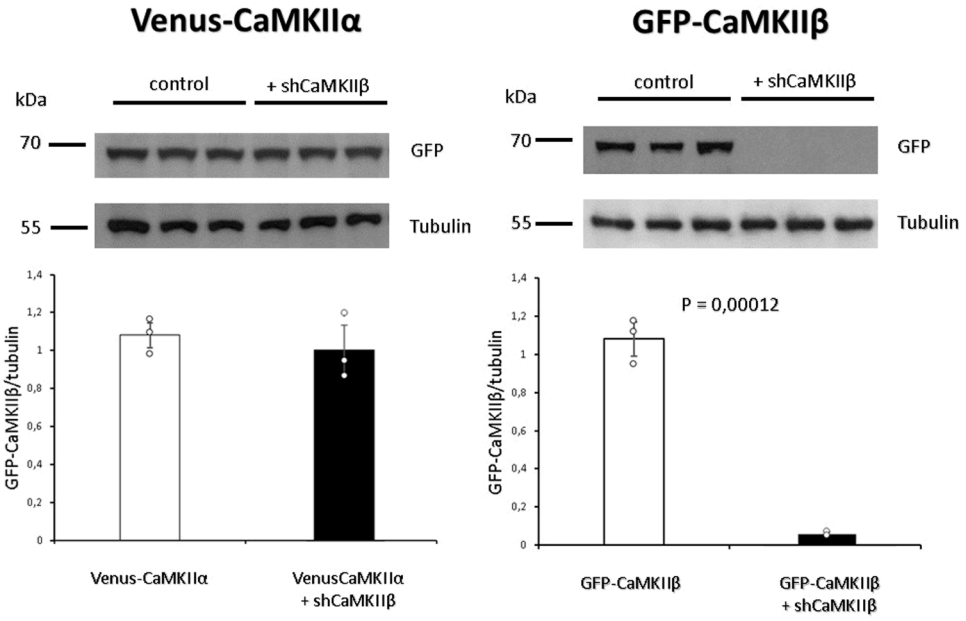

Fig. 3. Analysis of the specificity and effectiveness of CaMKIIβ knockdown in HEK293T cells. Western blot analysis of the expression of Venus-CaMKIIα (A) and GFP-CaMKIIβ (B) proteins in HEK293T cell lysates after co-transfection with Venus-CaMKIIα or GFP-CaMKIIβ plasmids together with either plasmid encoding control shRNA (shControl), or shRNA specific for CaMKIIβ (shCaMKIIβ). Quantitative analysis of the expression of Venus-CaMKIIα (C) and GFP-CaMKIIβ (D) on Western blot results depicted on panels A and B. The expression levels of the proteins are normalized to tubulin. Results are presented as mean ± SEM with individual data points. Statistical analysis was performed using Student's t-test, p value is indicated on the figure. Each band corresponds to a cell lysate taken from single well of 24 well plate.

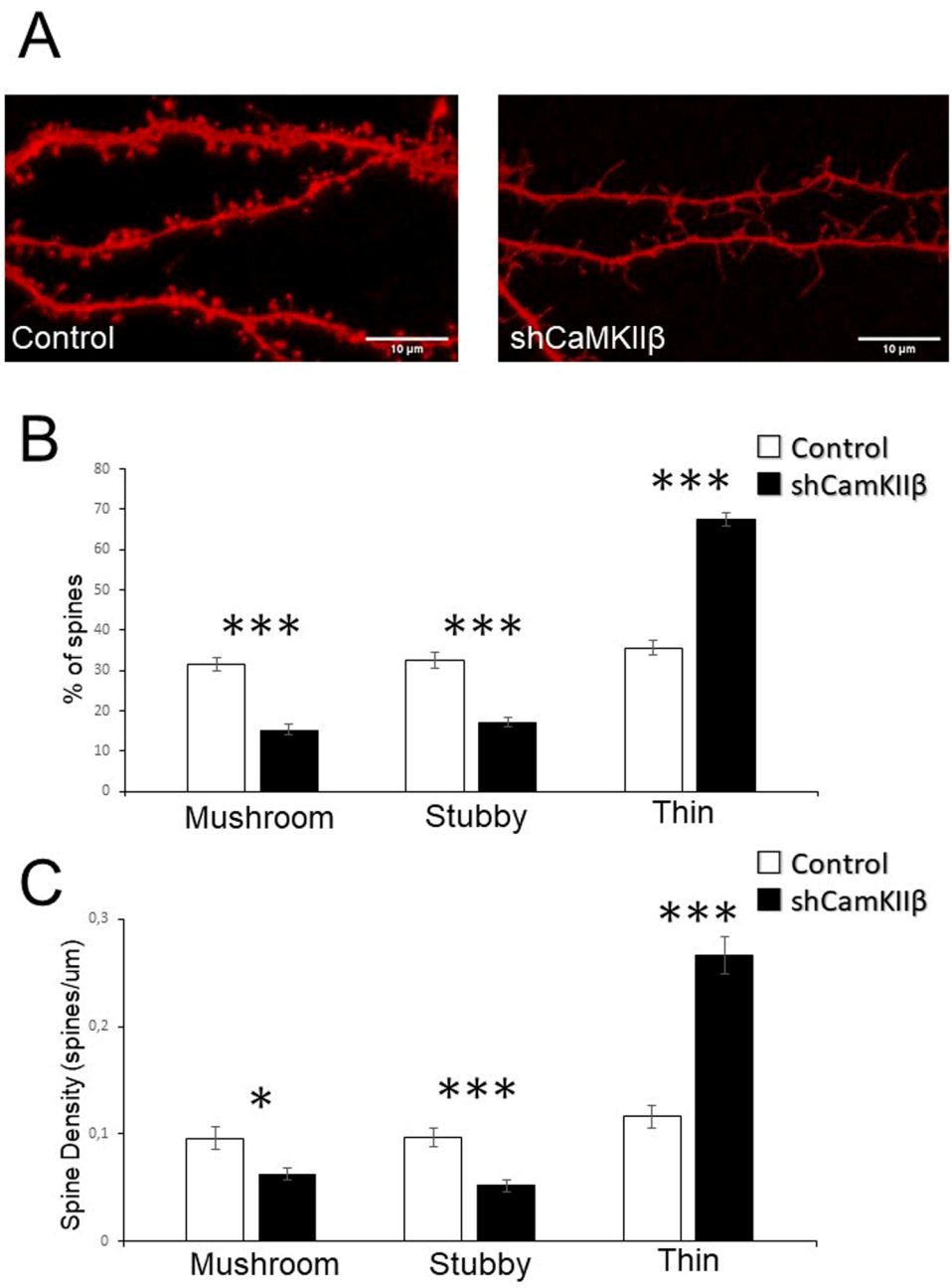

Fig. 4. CaMKIIβ knockdown causes mushroom and stubby spines loss and increases percentage of thin spines in hippocampal cultures. (A) representative confocal images of dendritic spines in control neurons (Control, co-transfected with TD-Tomato and shControl plasmids) and in neurons with CaMKIIβ knockdown (co-transfected with TD-Tomato and shCaMKIIβ plasmids). Histograms with average percentages (B) and spine densities (C) of mushroom, stubby and thin spines in two experimental groups, control neurons and in neurons with CaMKIIβ knockdown (shCaMKIIβ), quantified with Neuronstudio. Results are presented as mean ± SEM, experiments were repeated at least 4 times. n (neurons) ≥ 27. Statistical analysis was performed using Student's t-test, * $p < 0.05$, *** $p < 0.0001$. Scale bar = 10 μm.

knockdown effect on dendritic spines (Fink et al., 2003; Okamoto et al., 2007; Thiagarajan et al., 2002).

3.5. Knockdown of CaMKIIβ causes a decrease in nSOCE in dendritic spines in primary hippocampal cultures

To investigate the role of CaMKIIβ in regulation of nSOCE activity, we have performed calcium imaging experiments in primary hippocampal cultures co-transfected with GCamp5.3 and shCaMKIIβ plasmids. Control experiments were performed with neurons transfected with GCamp5.3 and shControl plasmids. The culture was transfected at DIV7 and the experiment was carried out a week later.

The experimental results are shown on Fig. 5. In contrast to Fluo 4 staining, GCamp5.3 is expressed in all parts of neurons, so in the representative graphs (Fig. 5 (A)) each gray curve corresponds to the value of one spine.

On average, the peak amplitude of nSOCE was equal to 9.58 ± 0.30 a.u. (n (spines) = 107) in shControl and GCamp5.3 co-transfected cultures and 5.45 ± 0.19 a.u. (n (spines) = 109) in hippocampal cultures co-transfected with shCaMKIIβ and GCamp5.3, $p < 0.0001$ (Fig. 5(B)). From these experiments we concluded that knockdown of CaMKIIβ causes decrease in nSOCE in dendritic spines of hippocampal neurons.

4. Discussion

Within the current study we have shown that CaMKII is involved in the regulation of nSOCE under conditions of primary hippocampal culture. It was established for the first time that pharmacological blocking of CaMKII activity by KN-62 causes a statistically significant decrease in the amplitude of nSOCE in the soma of hippocampal neurons (Fig. 2). This effect is probably associated with the participation of CaMKII in TRPC6 phosphorylation, which provides upregulation of TRPC6 (Shi et al., 2004, 2013). It is interesting that CaMKII inhibition by KN-62

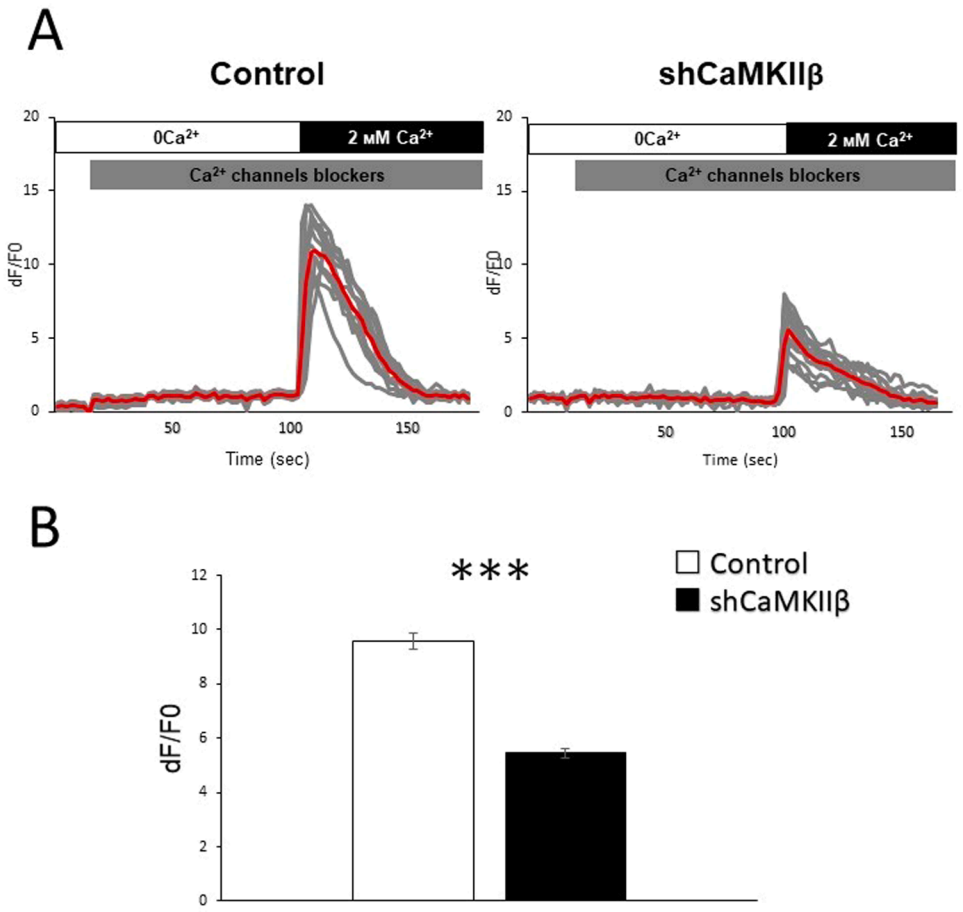

Fig. 5. CaMKIIβ knockdown decreases store-operated calcium entry in postsynaptic spines in primary hippocampal cultures. (A) Time course of GCaMP5.3 relative fluorescence signal changes (F/F0) in individual spines of hippocampal neurons. Presence of Ca^{2+} channels blockers (Tg, TTX, Nifedipine, D-AP5, CNQX) is indicated by grey bars. The time of extracellular Ca^{2+} readdition is indicated by a black bar above the traces. Neurons were co-transfected with either shControl + GCamp5.3(Control) or shCaMKIIβ+ GCamp5.3 (shCaMKIIβ) plasmids. For each experimental group, individual spine (gray) and average (red) fluorescence traces are shown. (B), Average nSOCE spine peak amplitude is shown for each group of cells shown in A panel. Mean F/F0 peak amplitude signals for each group are presented as mean ± SEM ($n \geq 107$ spines from 3 independent experiment). Statistical analysis was performed using Student's t-test, *** $p < 0.0001$.

mimics the effect of reduced TRPC6 expression or activity upon complement stimulation of podocytes (Kistler et al., 2013). At this part of experiments, we cannot differentiate which CaMKII isoform plays role in nSOCE downregulation since KN-62 blocks activity of all CaMKII isoforms identically (Tokumitsu et al., 1990). In the current paper we have shown for the first time that the knockdown of CaMKIIβ by RNA interference causes a decrease in the amplitude of nSOCE in the dendritic spines of hippocampal neurons (Fig. 5). The latter effect is probably associated with a decrease in the size of the head of dendritic spines caused by the reorganization of the actin cytoskeleton due to the absence of CaMKIIβ. In the present work, a decrease in the percentage of mushroom spines in the culture of neurons with CaMKIIβ knockdown was found (Fig. 4).

There are data confirming that CaMKIIβ is responsible for maintaining the spine structure. When CaMKIIβ is activated by calcium influx it separates from F-actin and allows filaments' reorganization by G proteins. Such reorganization increases the volume of the spine head. After neuronal activation non-phosphorylated CaMKII molecules again bind the newly reorganized F-actin. Thus, the new spine structure is maintained (Okamoto et al., 2007). This "gating" role of CaMKII in structural plasticity may explain our results.

In addition, our results are consistent with the previous studies of the effect of CaMKIIδ knockdown on SOCE. The knockdown of this subunit causes SOCE decrease in HEK293 and HeLa cells (Li et al., 2018).

Based on our data, it can be assumed that the effect of CaMKIIβ knockdown on nSOCE amplitude is associated with a decrease in the size of the spine head, due to the structural role of CaMKIIβ. As well as CaMKII might play a role in TRPC6 phosphorylation that is needed to support TRPC6 channel opening. In the future studies it might be interesting to investigate whether CaMKII participates in TRPC6 phosphorylation in hippocampal neurons. If it plays a role then it is interesting to investigate which isoform of CaMKII plays major mission in TRPC6 phosphorylation, at what positions and how it influences opening state of TRPC6.

CRediT authorship contribution statement

Nikita Zernov: Investigation, Methodology, Data curation, Software, Visualization, Writing – original draft. **Ilya Bezrpozvanny**: Writing – review, Project administration, Supervision. **Elena Popugaeva**: Conceptualization, Validation, Funding acquisition, Writing – review & editing.

Declarations of interest

None.

Acknowledgments

We thank Dr. A. Bolshakova for administrative support. Dr. Ilya Bezprozvanny is a holder of the Carl J. and Hortense M. Thomsen Chair in Alzheimer's Disease Research. This work was supported by Russian Science Foundation Grant No. 18–74-00027 (results depicted on Figs. 1 and 2) and by Russian Science Foundation Grant No. 20–75-10026 (results depicted on Figs. 3–5).

Appendix A. Supporting information

Supplementary data associated with this article can be found in the online version at doi:10.1016/j.ibneur.2022.01.001.

References

Bennett, M.K., Erondu, N.E., Kennedy, M.B., 1983. Purification and characterization of a calmodulin-dependent protein kinase that is highly concentrated in brain. J. Biol. Chem. 258 (20), 12735–12744. https://doi.org/10.1016/s0021-9258(17)44239-6.

Boros, B.D., Greathouse, K.M., Gentry, E.G., Curtis, K.A., Birchall, E.L., Gearing, M., Herskowitz, J.H., 2017. Dendritic spines provide cognitive resilience against Alzheimer's disease. Ann. Neurol. 82 (4), 602–614. https://doi.org/10.1002/ana.25049.

Bourne, J., Harris, K.M., 2007. Do thin spines learn to be mushroom spines that remember? Curr. Opin. Neurobiol. Vol. 17 (Issue 3), 381–386. https://doi.org/10.1016/j.conb.2007.04.009.

Castellani, R.J., Perry, G., 2012. Pathogenesis and Disease-modifying Therapy in Alzheimer's Disease: The Flat Line of Progress. Arch. Med. Res. 43 (8), 694–698. https://doi.org/10.1016/J.ARCMED.2012.09.009.

Chernyuk, D., Zernov, N., Kabirova, M., Bezprozvanny, I., Popugaeva, E., 2019. Antagonist of neuronal store-operated calcium entry exerts beneficial effects in neurons expressing PSEN1ΔE9 mutant linked to familial Alzheimer disease. Neuroscience. https://doi.org/10.1016/j.neuroscience.2019.04.043.

Emilsson, L., Saetre, P., Jazin, E., 2006. Alzheimer's disease: MRNA expression profiles of multiple patients show alterations of genes involved with calcium signaling. Neurobiol. Dis. 21 (3), 618–625. https://doi.org/10.1016/j.nbd.2005.09.004.

Fink, C.C., Bayer, K.U., Myers, J.W., Ferrell, J.E., Schulman, H., Meyer, T., 2003. Selective regulation of neurite extension and synapse formation by the β but not the α isoform of CaMKII. Neuron 39 (2), 283–297. https://doi.org/10.1016/S0896-6273(03)00428-8.

Gruszczynska-Biegala, J., Pomorski, P., Wisniewska, M.B., Kuznicki, J., 2011. Differential roles for STIM1 and STIM2 in store-operated calcium entry in rat neurons. PLoS One 6 (4). https://doi.org/10.1371/journal.pone.0019285.

Hayashi, Y., Majewska, A.K., 2005. Dendritic spine geometry: Functional implication and regulation. Neuron Vol. 46 (Issue 4), 529–532. https://doi.org/10.1016/j.neuron.2005.05.006.

Helm, M., Dankovich, T., Mandad, S., Rammner, B., Jähne, S., Salimi, V., Koerbs, C., Leibrandt, R., Urlaub, H., Schikorski, T., Rizzoli, S., 2021. A large-scale nanoscopy and biochemistry analysis of postsynaptic dendritic spines. Nat. Neurosci. 24 (8), 1151–1162. https://doi.org/10.1038/S41593-021-00874-W.

Hoffman, L., Farley, M.M., Waxham, M.N., 2013. Calcium-calmodulin-dependent protein kinase II isoforms differentially impact the dynamics and structure of the actin cytoskeleton. Biochemistry 52 (7), 1198–1207. https://doi.org/10.1021/bi3016586.

Ito, E., Oka, K., Etcheberrigaray, R., Nelson, T.J., McPhie, D.L., Tofel-Grehl, B., Gibson, G.E., Alkon, D.L., 1994. Internal Ca2+ mobilization is altered in fibroblasts from patients with Alzheimer disease. Proc. Natl. Acad. Sci. U. S. A. 91 (2), 534–538. https://doi.org/10.1073/pnas.91.2.534.

Kistler, A.D., Singh, G., Altintas, M.M., Yu, H., Fernandez, I.C., Gu, C., Wilson, C., Srivastava, S.K., Dietrich, A., Walz, K., Kerjaschki, D., Ruiz, P., Dryer, S., Sever, S., Dinda, A.K., Faul, C., Reiser, J., 2013. Transient Receptor Potential Channel 6 (TRPC6) Protects Podocytes during Complement-mediated Glomerular Disease *. J. Biol. Chem. 288 (51), 36598–36609. https://doi.org/10.1074/JBC.M113.488122.

Klejman, M.E., Gruszczynska-Biegala, J., Skibinska-Kijek, A., Wisniewska, M.B., Misztal, K., Blazejczyk, M., Bojarski, L., Kuznicki, J., 2009. Expression of STIM1 in brain and puncta-like co-localization of STIM1 and ORAI1 upon depletion of Ca2+ store in neurons. Neurochem. Int. 54 (1), 49–55. https://doi.org/10.1016/j.neuint.2008.10.005.

LaFerla, F.M., 2002. Calcium dyshomeostasis and intracellular signalling in alzheimer's disease. Nat. Rev. Neurosci. 3 (11), 862–872. https://doi.org/10.1038/nrn960.

Li, S., Xue, J., Sun, Z., Liu, T., Zhang, L., Wang, L., You, H., Fan, Z., Zheng, Y., Luo, D., 2018. CaMKII Potentiates Store-Operated Ca 2+ Entry Through Enhancing STIM1 Aggregation and Interaction with Orai1. Cell. Physiol. Biochem. 46 (3), 1042–1054. https://doi.org/10.1159/000488835.

Ng, A.N., Krogh, M., Toresson, H., 2011. Dendritic EGFP-STIM1 activation after type I metabotropic glutamate and muscarinic acetylcholine receptor stimulation in hippocampal neuron. J. Neurosci. Res. 89 (8), 1235–1244. https://doi.org/10.1002/JNR.22648.

O'Leary, H., Lasda, E., Bayer, K.U., 2006. CaMKIIβ association with the actin cytoskeleton is regulated by alternative splicing. Mol. Biol. Cell 17 (11), 4656–4665. https://doi.org/10.1091/mbc.E06-03-0252.

Okamoto, K.I., Narayanan, R., Lee, S.H., Murata, K., Hayashi, Y., 2007. The role of CaMKII as an F-actin-bundling protein crucial for maintenance of dendritic spine structure. Proc. Natl. Acad. Sci. U. S. A. 104 (15), 6418–6423. https://doi.org/10.1073/pnas.0701656104.

Popugaeva, E., Chernyuk, D., Zhang, H., Postnikova, T.Y., Pats, K., Fedorova, E., Poroikov, V., Zaitsev, A.V., Bezprozvanny, I., 2019. Derivatives of Piperazines as Potential Therapeutic Agents for Alzheimer's Disease. Mol. Pharmacol. 95 (4), 337–348. https://doi.org/10.1124/mol.118.114348.

Popugaeva, E., Pchitskaya, E., Bezprozvanny, I., 2018. Dysregulation of Intracellular Calcium Signaling in Alzheimer's Disease. Antioxidants Redox Signal. 29 (12), 1176. https://doi.org/10.1089/ARS.2018.7506.

Popugaeva, E., Pchitskaya, E., Speshilova, A., Alexandrov, S., Zhang, H., Vlasova, O., Bezprozvanny, I., 2015. STIM2 protects hippocampal mushroom spines from amyloid synaptotoxicity. Mol. Neurodegen. 10 (1), 37. https://doi.org/10.1186/s13024-015-0034-7.

Redondo, R.L., Okuno, H., Spooner, P.A., Frenguelli, B.G., Bito, H., Morris, R.G.M., 2010. Synaptic tagging and capture: Differential role of distinct calcium/calmodulin kinases in protein synthesis-dependent long-term potentiation. J. Neurosci. 30 (14), 4981–4989. https://doi.org/10.1523/JNEUROSCI.3140-09.2010.

Rodriguez, A., Ehlenberger, D.B., Dickstein, D.L., Hof, P.R., Wearne, S.L., 2008. Automated three-dimensional detection and shape classification of dendritic spines from fluorescence microscopy images. PLoS One 3 (4). https://doi.org/10.1371/journal.pone.0001997.

Ryskamp, D., Wu, L., Wu, J., Kim, D., Rammes, G., Geva, M., Hayden, M., Bezprozvanny, I., 2019. Pridopidine stabilizes mushroom spines in mouse models of Alzheimer's disease by acting on the sigma-1 receptor. Neurobiol. Dis. 124, 489–504. https://doi.org/10.1016/j.nbd.2018.12.022.

Shen, K., Teruel, M.N., Subramanian, K., Meyer, T., 1998. CaMKIIβ functions as an F-actin targeting module that localizes CaMKIIα/β heterooligomers to dendritic spines. Neuron 21 (3), 593–606. https://doi.org/10.1016/S0896-6273(00)80569-3.

Shi, J., Geshi, N., Takahashi, S., Kiyonaka, S., Ichikawa, J., Hu, Y., Mori, Y., Ito, Y., Inoue, R., 2013. Molecular determinants for cardiovascular TRPC6 channel regulation by Ca 2+ /calmodulin-dependent kinase II. The Authors. J. Physiol. C 591, 2851–2866. https://doi.org/10.1113/jphysiol.2013.251249.

Shi, J., Mori, E., Mori, Y., Mori, M., Li, J., Ito, Y., Inoue, R., 2004. Multiple regulation by calcium of murine homologues of transient receptor potential proteins TRPC6 and TRPC7 expressed in HEK293 cells. J. Physiol. 561 (2), 415–432. https://doi.org/10.1113/jphysiol.2004.075051.

Skibinska-Kijek, A., Wiśniewska, M., Gruszczynska-Biegala, J., Methner, A., & Kuźnicki, J. (2009). Immunolocalization of STIM 1 in the mouse brain.

Sun, S., Zhang, H., Liu, J., Popugaeva, E., Xu, N.J., Feske, S., White, C.L., Bezprozvanny, I., 2014. Reduced synaptic STIM2 expression and impaired store-operated calcium entry cause destabilization of mature spines in mutant presenilin mice. Neuron 82 (1), 79–93. https://doi.org/10.1016/j.neuron.2014.02.019.

Supnet, C., Bezprozvanny, I., 2010. The dysregulation of intracellular calcium in Alzheimer disease. In: Cell Calcium, Vol. 47. Elsevier Ltd,, pp. 183–189. https://doi.org/10.1016/j.ceca.2009.12.014.

Tackenberg, C., Ghori, A., Brandt, R., 2009. Thin, stubby or mushroom: spine pathology in Alzheimers disease. Curr. Alzheimer Res. 6 (3), 261–268. https://doi.org/10.2174/156720509788486554.

Thaler, S.V., K, H.L., P, P.S., B, SS, V., 2009. Structural rearrangement of CaMKIIalpha catalytic domains encodes activation. Proc. Natl. Acad. Sci. U. S. A. 106 (15), 6369–6374. https://doi.org/10.1073/PNAS.0901913106.

Thiagarajan, T.C., Piedras-Renteria, E.S., Tsien, R.W., 2002. α- and βCaMKII: Inverse regulation by neuronal activity and opposing effects on synaptic strength. Neuron 36 (6), 1103–1114. https://doi.org/10.1016/S0896-6273(02)01049-8.

Tobimatsu, T., Fujisawa, H., 1989. Tissue-specific expression of four types of rat calmodulin-dependent protein kinase II mRNAs. J. Biol. Chem. 264 (30), 17907–17912. https://doi.org/10.1016/s0021-9258(19)84658-6.

Tokumitsu, H., Chijiwa, T., Hagiwara, M., Mizutani, A., Terasawa, M., Hidaka, H., 1990. KN-62, 1-[N,O-Bis(5-isoquinolinesulfonyl)-N-methyl-L-tyrosyl]-4-phenylpiperaz ine, a specific inhibitor of Ca2+/calmodulin-dependent protein kinase II. J. Biol. Chem. 265 (8), 4315–4320. https://doi.org/10.1016/s0021-9258(19)39565-1.

Tønnesen, J., Katona, G., Rózsa, B., Nägerl, U.V., 2014. Spine neck plasticity regulates compartmentalization of synapses. Nat. Neurosci. 17 (5), 678–685. https://doi.org/10.1038/nn.3682.

Vlachos, A., Korkotian, E., Schonfeld, E., Copanaki, E., Deller, T., Segal, M., 2009. Synaptopodin regulates plasticity of dendritic spines in hippocampal neurons. J. Neurosci.: Off. J. Soc. Neurosci. 29 (4), 1017–1033. https://doi.org/10.1523/JNEUROSCI.5528-08.2009.

Waldner, W., M, R., GU, R., 2009. Red fluorescent Xenopus laevis: a new tool for grafting analysis. BMC Dev. Biol. 9 (1) https://doi.org/10.1186/1471-213X-9-37.

Zhang, H., Wu, L., Pchitskaya, E., Zakharova, O., Saito, T., Saido, T., Bezprozvanny, I., 2015. Neuronal store-operated calcium entry and mushroom spine loss in amyloid precursor protein knock-in mouse model of Alzheimer's disease. J. Neurosci. https://doi.org/10.1523/jneurosci.1034-15.2015.

Zhang, Hua, Sun, S., Wu, L., Pchitskaya, E., Zakharova, O., Fon Tacer, K., Bezprozvanny, I., 2016. Store-operated calcium channel complex in postsynaptic spines: a new therapeutic target for Alzheimer's disease treatment. J. Neurosci. 36 (47), 11837–11850. https://doi.org/10.1523/JNEUROSCI.1188-16.2016.